

## The Determination of the Efficiency of Energy Dispersive X-Ray Spectrometers by a New Reference Material

Marco Alvisi,<sup>1</sup> Markus Blome,<sup>2</sup> Michael Griepentrog,<sup>3</sup> Vasile-Dan Hodoroaba,<sup>3</sup> Peter Karduck,<sup>2</sup> Marco Mostert,<sup>4</sup> Michele Nacucchi,<sup>1</sup> Mathias Procop,<sup>3,\*</sup> Martin Rohde,<sup>5</sup> Frank Scholze,<sup>6</sup> Peter Statham,<sup>7</sup> Ralf Terborg,<sup>5</sup> and Jean-Francois Thiot<sup>4</sup>

<sup>1</sup>ENEA, Research Centre of Brindisi, S.S. 7 Appia km 713.7, I-72100 Brindisi, Italy

<sup>2</sup>HDZ Herzogenrather Dienstleistungszentrum GbR, Kaiserstrasse 100, D-52134 Herzogenrath, Germany

<sup>3</sup>Bundesanstalt fuer Materialforschung und -pruefung (BAM), D-12200 Berlin, Germany

<sup>4</sup>SAMx, 1554 route de la Roquette, F-06670 Levens, France

<sup>5</sup>Roentec, Schwarzschildstrasse 12, D-12489 Berlin, Germany

<sup>6</sup>Physikalisch-Technische Bundesanstalt, Abbestraße 2-12, 10587 Berlin, Germany

<sup>7</sup>Oxford Instruments Analytical Limited, Halifax Road, High Wycombe, Bucks HP12 3SE, UK

**Abstract:** A calibration procedure for the detection efficiency of energy dispersive X-ray spectrometers (EDS) used in combination with scanning electron microscopy (SEM) for standardless electron probe microanalysis (EPMA) is presented. The procedure is based on the comparison of X-ray spectra from a reference material (RM) measured with the EDS to be calibrated and a reference EDS. The RM is certified by the line intensities in the X-ray spectrum recorded with a reference EDS and by its composition. The calibration of the reference EDS is performed using synchrotron radiation at the radiometry laboratory of the Physikalisch-Technische Bundesanstalt. Measurement of RM spectra and comparison of the specified line intensities enables a rapid efficiency calibration on most SEMs. The article reports on studies to prepare such a RM and on EDS calibration and proposes a methodology that could be implemented in current spectrometer software to enable the calibration with a minimum of operator assistance.

**Key words:** energy dispersive X-ray spectrometry, standardless analysis, X-ray detectors, detection efficiency, spectrometer calibration

### INTRODUCTION

Electron probe X-ray microanalysis (EPMA) is applied to determine the concentration of chemical elements in a microscopic volume of a specimen. In many cases analysis is performed by means of an energy dispersive X-ray spectrometer (EDS) attached to a scanning electron microscope (SEM). Physical equations relate the element concentrations to the number of emitted photons. A long-term goal of X-ray microanalysis is to calculate the concentrations without the additional need to measure spectra from standard specimens. The accuracy of so-called standardless analysis has been repeatedly discussed at EMAS workshops (Pouchou, 1994; Wernisch & Röhrbacher, 1998; Joy, 2002). However, little attention has been paid to the spectrometer efficiency, which is the critical factor relating the counts measured by the EDS to the number of photons emitted toward the detector entrance window. This relation is defined as spec-

trometer efficiency and must be known for standardless analysis.

The spectrometer efficiency depends strongly on photon energy. It is usually calculated from X-ray absorption of the individual detector components (window, front contact, crystal material). Some layer thicknesses are not known with sufficient accuracy to calculate exactly the efficiency for an individual spectrometer. In addition, the efficiency may change during spectrometer operation due to buildup of contamination layers on the detector or by degradation. Hence, when spectrometer efficiency is calculated from assumed data for the detector design, considerable errors can be involved. This study explores the feasibility of measuring spectrometer efficiency by means of an easy methodology. The basic idea is to find the unknown spectrometer efficiency by comparison of two spectra from a reference material (RM). One spectrum is measured with the spectrometer of unknown efficiency, the other one with a spectrometer of known efficiency, that is, with a calibrated reference spectrometer. In the following, the notation “unknown spectrometer” stands for the spectrometer with unknown efficiency, and “efficiency transfer” means the procedure to get the unknown efficiency by comparison of the RM X-ray spectra.

The present work describes the selection of the RM, which is specified mainly by its X-ray spectrum. The preparation as a thick film and its characterization concerning chemical composition, structure, and stability are given. A short outline of the determination of the efficiency of the reference spectrometer using synchrotron radiation (SR) is followed by the explanation of the efficiency transfer procedure to get the efficiency for an unknown spectrometer. A methodology that can be applied to most SEM/EDS systems is proposed. Finally, examples of the efficiency transfer are presented, and its precision is estimated.

## MATERIALS AND METHODS

### Requirements for the Reference Material

The reference material should meet the following requirements with respect to X-ray spectroscopy:

1. It should contain different chemical elements emitting characteristic X-ray lines in a wide energy range from about 0.2 to 20 keV. X-ray lines should be preferably positioned at energies close to (below or above) absorption edges in the efficiency curve of the EDS detector to distinguish the effects of different absorbing materials on efficiency. The X-ray lines should be separated at least by two times the full width at half maximum (FWHM) to enable a robust background subtraction method and to avoid an uncertainty in peak area determination caused by deconvolution.
2. The peak-to-background ratio for characteristic peaks should be high to maximize the precision that can be obtained in an acceptable measurement time.
3. The intensities of the strongest X-ray lines should be similar to balance the precision of measurement throughout the energy range.

In addition, the requirements related to materials properties and stability are:

1. The surface should be smooth and flat to have a well-defined take-off angle (TOA). The RM should be large in diameter (at least 20 mm) to enable accurate adjustment of surface tilt in the SEM.
2. The RM must be laterally homogeneous in order to make the result of the efficiency calibration independent of the position on the specimen surface. A homogeneous region of about 100 mm<sup>2</sup> in the center of each sample would be sufficient for the application. In-depth homogeneity is required for the application of the EPMA absorption correction formalism when spectra from unknown and calibrated reference spectrometers are measured at different TOAs.
3. The electrical conductivity should allow electron bombardment without any charging of the material.

4. The material should not suffer any changes in morphology and surface composition or show any other damage under electron bombardment.
5. It should be stable over longer periods of storage under laboratory conditions, that is, undergo no phase transitions, precipitations, other decompositions, or remarkable reactions with atmosphere (oxidation).
6. Finally, the preparation technique must be reproducible and capable of a sufficiently high production or repetition rate to provide large numbers of specimens for specification or certification.

The selection, preparation, and characterization of a material that fulfills all these requirements are described later in the Results section.

### Efficiency of Energy Dispersive Spectrometers

The spectrometer efficiency, defined above as the probability that an incoming photon is detected as a pulse by the spectrometer, is given by the following equation, which holds for spectrometers with semiconductor detector and thin film window:

$$\varepsilon_{tot} = \prod_w \exp(-\mu_w d_w) \cdot [T + (1 - T) \exp(-\mu_{Si} d_{sg})] \cdot \exp(-\mu_c d_c) \exp(-\mu_{dl} d_{dl}) (1 - \exp(-\mu_{sc} d_{sc})) \times (1 + \sigma_i). \quad (1)$$

The first factor describes the absorption by the foil of the window. The index  $w$  covers all the elements present in the foil.  $\mu_w$  denotes their mass absorption coefficients (MAC) and  $d_w$  their mass thicknesses. The second factor is the transmission through the support of the foil, which is typically a 0.38-mm-thick silicon supporting grid ( $d_{sg}$ ) with a geometrical transparency  $T$  between 0.75 and 0.8. The remaining factors give the transmission through the front contact, the dead layer, and the absorption in the semiconducting detector crystal itself.  $\mu$  and  $d$  stand again for corresponding absorption coefficients and thicknesses. Equation (1) also applies to detectors with beryllium windows. In this case  $T$  is equal to one. A minor contribution  $\sigma_i$  is added in equation (1) to take into account pulses caused by the injection of photoelectrons and Auger electrons into the active volume of the detector crystal. They are generated by photoabsorption in a very narrow region either of the dead layer or, in case of a Schottky diode, of the front contact adjacent to the active volume (Goto, 1993; Scholze & Ulm, 1994; Lowe, 2000). The MACs  $\mu$  and  $\sigma_i$  are functions of the photon energy  $E_{ph}$ .

Equation (1) gives the *total efficiency*. It does not consider in which channel of the multichannel analyzer of the spectrometer the pulse is sorted. However, even an incident monochromatic radiation gives a spectrum with a main peak, an escape peak, sum peaks, and a shelf, whereas the

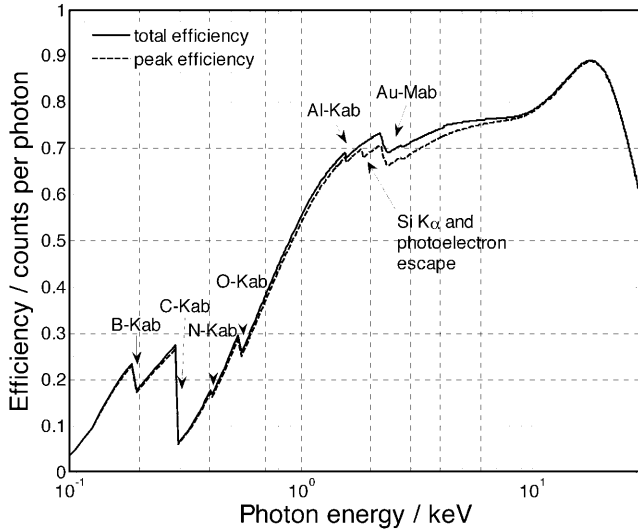


**Figure 1.** Efficiency of a typical 3-mm-thick Si(Li) detector with 20 nm Au front contact, no dead layer, and Moxtek AP3.3 window.

main peak consists of a Gaussian part and a low-energy tail. This spectrum is denoted as the response function (Campbell et al., 1987). In Energy Dispersive Electron Microprobe Analysis (ED-EPMA), only the pulses in the main peak are used to measure the intensity of an emitted X-ray line. This means that for standardless analysis a *peak efficiency* must be known. Assuming that the processor is fast enough so that dead time is low and sum peaks can be neglected, the peak efficiency is given by

$$\begin{aligned} \varepsilon_{peak} = & \prod_w \exp(-\mu_w d_w) \cdot [T + (1 - T) \exp(-\mu_{Si} d_{sg})] \\ & \cdot \exp(-\mu_c d_c) \exp(-\mu_{Al} d_{Al}) (1 - \exp(-\mu_{sc} d_{sc})) \\ & \times (1 - \eta)(1 - \sigma_e), \end{aligned} \quad (2)$$

where  $\eta$  is the escape probability, which can be calculated (Reed & Ware, 1972), and  $\sigma_e$  considers the loss of pulses in the main peak due to emission of photoelectrons and Auger electrons out from the active region of the semiconductor crystal. Figure 1 compares total and peak efficiency calculated for a 3-mm-thick Si(Li) detector with 20 nm Au front contact and with a Moxtek AP3.3 window as an example. The difference is caused by the escape effect, which reduces the peak efficiency for  $E_{ph} > 1.84$  keV, and by the shelf, that is, the sum of  $\sigma_i + \sigma_e$ .

### Calibration of Efficiency

Two measurement schemes were applied as sketched in Figure 2. In the first scheme the EDS is exposed to the undispersed, direct SR of a bending magnet. Because the direct SR spectrum can be calculated from stored electron current, electron kinetic energy, magnetic field strength,

and geometrical conditions like aperture size and distance (Schwinger, 1949), a storage ring is a primary source standard for radiation metrology (Ulm et al., 1998). For spectrometer calibration, the storage ring has to be operated in a special mode with only a few electrons stored instead of about  $10^{12}$  in normal high-flux operation (Scholze et al., 2001). Alternatively, the EDS can be placed behind a monochromator, and the photon flux behind the monochromator is determined by a reference detector. In this work, the energy range covered by the monochromator was 0.1–1.5 keV. Details on the experimental arrangement at BESSY II are given by Beckhoff et al. (2000).

From both kinds of measurements, the peak efficiency (equation (2)) can be derived (Scholze et al., 1996). The spectrum measured with the monochromator radiation corresponds to the response function. Normalization of the main peak to the photon flux gives the peak efficiency at the energy selected. To find the peak efficiency from the spectrum measured with undispersed radiation is more complicated. This spectrum is the product of the direct SR spectrum and the total spectrometer efficiency convoluted with the response function.

To get the peak efficiency, first the free parameters in a model describing tail and shelf were derived from the response functions measured with the monochromatic radiation (Scholze & Ulm, 1994). This model is similar to those of Goto (1993) and Lowe (2000). Second, using these parameters, the response functions for all spectrometer channels from 0.1 to 20 keV were derived to perform the convolution mentioned above. Third, absorbing layer thicknesses in equation (1) were varied until agreement between calculated and measured spectra has been achieved. Finally, the layer thicknesses found were used to calculate the peak efficiency according to equation (2) (Scholze & Procop, 2001).

Efficiency determination by undispersed SR is much faster than measurements with monochromatic radiation. It gives exact values for the mass thickness of front contact and aluminum window coating as well as grid opening  $T$ . At low photon energy, the measurement accuracy is limited by the energy resolution of EDS. Due to the proximity of the low-energy absorption edges, the different layer thicknesses particularly of the window foil cannot be uniquely determined from the measurement with undispersed SR. In this case the measurement with monochromatized SR gives more accurate results.

### Efficiency Transfer

Efficiency transfer was defined above as the calibration of the efficiency of the unknown spectrometer by means of the known efficiency of a calibrated reference spectrometer and the X-ray spectra from the RM measured with both instruments. For this we rely only on measurements performed in SEMs and on the utilization of an RM with properties as described above. Requirements for the SEMs and EDS sys-

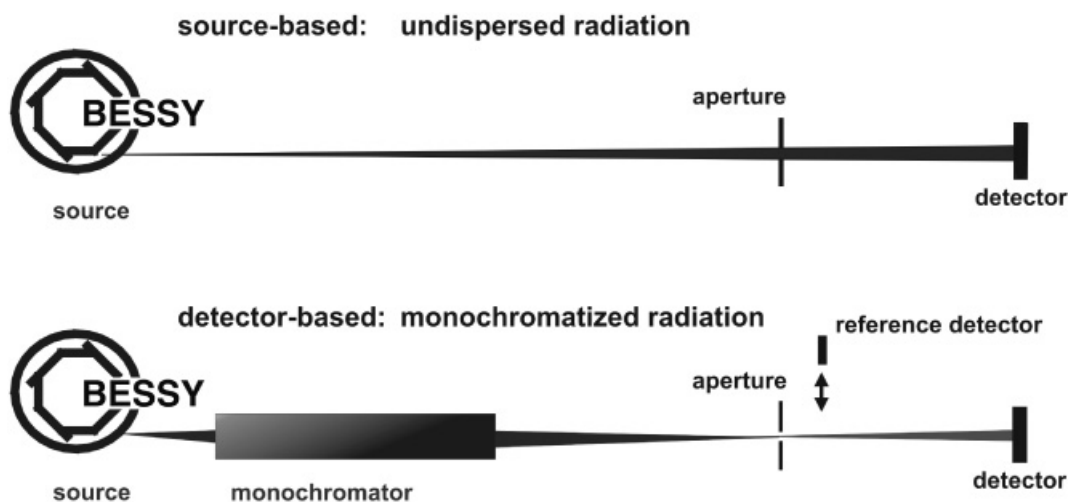


**Figure 2.** Schemes of the measurement setup for detector calibration. The upper scheme shows the measurement using the storage ring as a source standard; the lower scheme is the comparison of the detector to be calibrated to a detector standard.

tems to perform the efficiency transfer are the same as in quantitative ED-EPMA. However, for efficiency transfer, the accuracy of instrumental parameters (high voltage, TOA, and specimen tilt) should be checked very carefully to realize the targeted improvement in standardless analysis by using a calibrated spectrometer.

The efficiency  $\varepsilon^i$  of the unknown spectrometer at the energy of a characteristic line  $i$  is found from the intensity of the characteristic peak  $I^i$  in the spectra of the RM measured with the unknown and the reference spectrometer and the known efficiency  $\varepsilon_o^i$  of the reference spectrometer:

$$\varepsilon^i = c \frac{I^i}{I_o^i} \varepsilon_o^i.$$

The constant  $c$  accounts for different spectrum acquisition parameters: beam current, live time, and solid angle.  $c$  can be eliminated by normalization to a selected line  $n$ :

$$\varepsilon^i = \frac{\varepsilon^n}{\varepsilon_o^n} \frac{I^i/I^n}{I_o^i/I_o^n} \varepsilon_o^i. \quad (3)$$

When the line  $n$  is selected in the energy range between 5 and 10 keV, the influence of absorbing layers on the efficiency is negligible (see Fig. 1), and the term  $\varepsilon^n/\varepsilon_o^n$  reduces to the ratio of the grid openings  $T$  for both detectors. Therefore, in case of the same window type, the term is nearly one.

For standardless analysis, the spectrometer efficiency must be known for all energies in the range from 0.15 to 10 keV and in some cases up to 20 keV. To get the efficiency as a continuous function for this wide range, equation (2) is fitted to the  $\varepsilon^i$  values with the thicknesses as free parameters.

## RESULTS

### Preparation and Characterization of the RM

A suitable RM composition has been found to be an artificial mixture with the components carbon, aluminum, manganese, copper, and zirconium. It can be prepared by reactive cosputtering as thick layers on polished steel substrates. Disks 30 mm in diameter and 5 mm high allow convenient handling by the user. A layer thickness of about 10  $\mu\text{m}$  has been realized. This is sufficient to contain the complete excitation volume of characteristic lines for 30-keV primary electrons, so that it can be considered as bulk material. Figure 3 gives the 10-kV spectrum together with the efficiency of the spectrometer used for measurement.

The RM has been tested for thermal stability and stability against prolonged electron beam exposure. The as-deposited layers are amorphous and covered by an initial surface oxide layer of about 15-nm thickness. After thermal stress at 50°C or 100°C, only a slight but irrelevant increase of the oxide layer was found by electron spectroscopy. No growth of microcrystals could be observed by X-ray diffraction. The material has been found to be stable against electron beam exposure in the SEM and in the electron microprobe. This does not exclude that a carbon layer on the surface can be formed during measurement depending on vacuum quality in the SEM analysis chamber. A growing carbon layer must be avoided to get the correct C-K line intensity. Carbon layer buildup can be minimized by using a small raster scan rather than spot mode. The methodology proposed below recommends a raster scan of  $100 \times 100 \mu\text{m}^2$ . The RM homogeneous region of at least  $10 \times 10 \text{mm}^2$  enables repeated measurements at different virginal specimen locations. Moreover, the specimen can be cleaned in

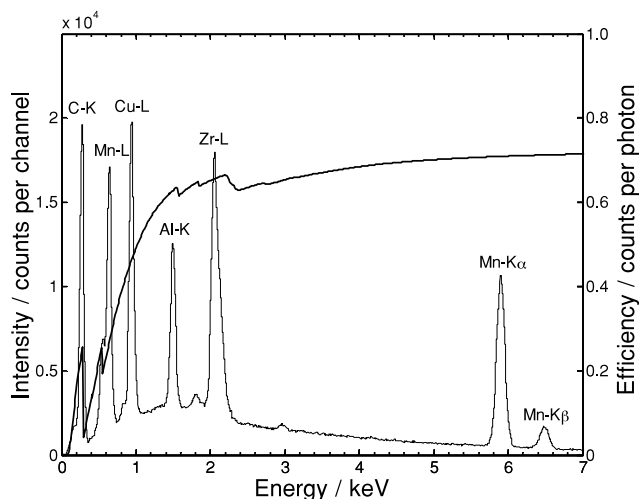


**Figure 3.** Measured 10-kV spectrum of the RM specimen and related spectrometer efficiency.

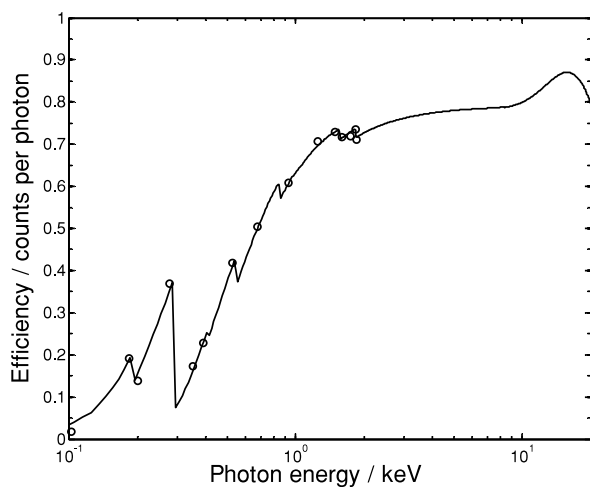


**Figure 4.** Measured peak efficiency using monochromatized SR (circles) and undispersed SR (solid line).

alcohol and washed in an ultrasonic bath. It can even be slightly polished because the about 10- $\mu\text{m}$ -thick film is extremely hard (Vickers hardness in the range of 1000). From experience with the handling of this kind of specimen and the results of the stability test, the estimated time period in which the specimen can be used in laboratory conditions is at least 1 year.

### Reference Spectrometer Calibration

In this study, four different spectrometers, three with a Si(Li) crystal and one with a silicon drift detector (SDD), were calibrated with SR. For all measurements, the photon flux was set to give a count rate of about 1000 cps at the longest shaping time and for a dead time below 30%.

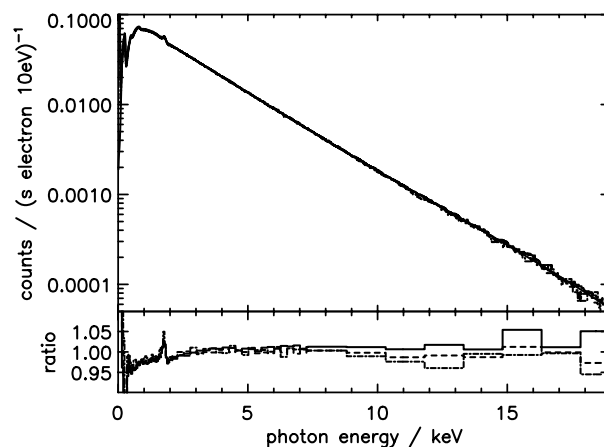


**Figure 5.** Measured spectra using undispersed radiation. Shown are measurements with 9.6 kcps (solid line), 4.8 kcps (dashed line), and 1.1 kcps (dash-dotted line). The lower panel shows the ratio between measurement and the spectrum calculated using the efficiency from the measurements with monochromatized radiation (see Fig. 4) and a response function model.

Figure 4 gives, as an example, the peak efficiency determined for one of the Si(Li) spectrometers using monochromatic SR. Spectra measured with undispersed radiation are shown in Figure 5. From these spectra, the peak efficiency was also calculated as described above. The combination of the two data sets yields reliable and accurate data for the whole energy range from 0.1 to 20 keV. The uncertainty is about 2% for photon energies up to 5 keV, as was shown in a previous work (Scholze & Procop, 2001). The results from both methods must agree to be sure that equations (1) and (2) can be applied. Otherwise, additional factors, not considered in these equations, influence the efficiency. The agreement was successfully verified for three of the four calibrated spectrometers. This is demonstrated for the example shown in Figure 4. For one of the spectrometers, the efficiency determined by the two approaches differed from each other at energies below 1 keV up to 30%, although count rate and shaping time were the same. Even the jump ratios for C-K and O-K deduced from the spectrum measured with undispersed radiation were in agreement with the result of the measurements with monochromatic radiation. It seems that for this spectrometer, the discriminator threshold depends on the pulse height distribution. The spectrometer is not suited as a reference spectrometer.

The method with undispersed radiation was also used to obtain information on the pulse-rate linearity and dead-time correction functionality of the spectrometer by comparison with spectra measured at higher count rates and shorter shaping times. For these measurements, the number of stored electrons in the storage ring was stepwise decreased, resulting in well-known ratios of the incident photon flux. By scaling the spectra to the same incident photon flux for each of the four spectrometers, a perfect match within the counting statistics was observed.

The exponential decay of the SR intensity with energy increased the uncertainty in efficiency determination using undispersed radiation for energies above 10 keV due to poor counting statistics. Therefore, energy intervals of about 1 keV were binned at high energies to improve the statistics. This is justified because the efficiency only weakly depends on energy in this range. The uncertainty of this approach was estimated from the lower panel in Figure 5. Here, statistical deviation of the measured spectrum from the model according to equation (1) is shown. For energies above 10 keV, the fluctuations strongly increase with photon energy and are about 5% at 17 keV.

### Methodology of Efficiency Transfer

A practical procedure that includes specimen handling (cleaning, mounting, storage) and spectrum measurement has been established and tested for several SEM/EDS systems. The procedure recommends measuring a 10-kV spectrum to get C-K, Mn-L, Cu-L, Al-K, Zr-L, and Mn-K $\alpha$  intensities and a 30-kV spectrum to obtain the Al-K, Zr-L, Mn-K $\alpha$ , Cu-K $\alpha$ , Zr-K $\alpha$ , and Zr-K $\beta$  intensities. Measurements shall be performed with the electron beam scanned over an area of  $0.1 \times 0.1 \text{ mm}^2$  at perpendicular incidence. To get reasonable counting statistics, spectrum accumulation shall not be stopped until about  $10^5$  counts in the C-K peak of the 10-kV spectrum, and about  $10^4$  counts in the Zr-K $\beta$  peak of the 30 kV spectrum were reached. Largest shaping time shall be selected for the 10-kV spectrum. The processor should be switched to a shorter shaping time to have a reasonable acquisition time also for the 30-kV spectrum.

Background subtraction has to be applied to get the line intensities as net peak areas. Correct net peak areas are very important for the efficiency transfer. Several methods for background removal were tested with simulated spectra, that is, with spectra for which the line intensities are known *a priori*. It has been found that the calculation of a physical background and a scaling of this background to the measured spectrum in peak-free regions give the best results in this special case where the composition of the specimen is known.

For the background construction, the following well-known expression was used:

$$B = F_s \varepsilon_{peak} \frac{E_0 - E}{E^{1.21}} F_a, \quad (4)$$

where  $F_s$  is a scaling factor and  $\varepsilon_{peak}$  is the spectrometer efficiency. The third factor describes the generated bremsstrahlung as proposed by Reed (1975). The last factor is the absorption correction where the Philibert expression (Philibert, 1963) has been used in this work. The scaling factor  $F_s$  cannot be assumed to be constant because the Reed and Philibert formulas are approximations with relatively large uncertainties at low energies. Moreover, both electron back-

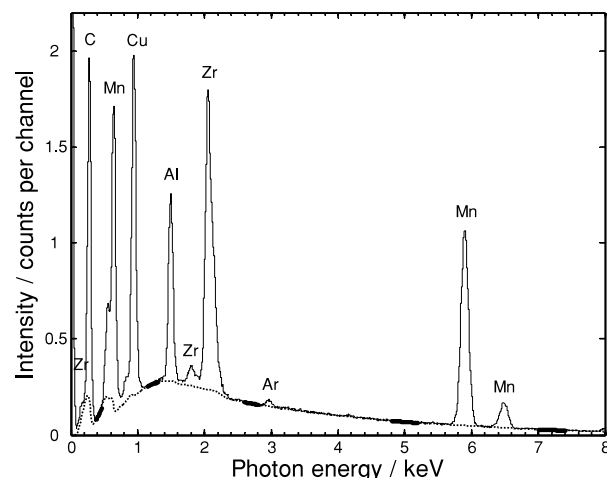


**Figure 6.** Measured 10-kV spectrum with constructed background (dotted) and regions for background scaling (bold).

scattering and the contribution of the shelf caused by the detector have been neglected in equation (4). Therefore, peak-free regions were defined to get  $F_s$  in these regions. In between,  $F_s$  was linearly interpolated. An example of background calculation for a 10-kV spectrum is given in Figure 6. The application of this procedure to simulated spectra, for which the net intensities and the shape of the bremsstrahlung spectrum are known *a priori*, demonstrated that net intensities could be found with an uncertainty of about 1%.

After measurement of the 10-kV and 30-kV spectra for both the calibrated and the unknown spectrometer and net peak area determination as described before, the efficiencies  $\varepsilon^i$  for the nine line energies are calculated from equation (3):

$$\varepsilon^i = \frac{\varepsilon^{Mn} I^i/I^{Mn}}{\varepsilon_0^{Mn} I_0^i/I_0^{Mn}} \varepsilon_0^i. \quad (5)$$

Line intensities were normalized in equation (5) to Mn-K $\alpha$ . This line has a high intensity in both the 10-kV spectrum and the 30-kV spectrum. For the Mn-K $\alpha$  line energy, the absorption factors in equation (2) are close to one and the efficiency ratio  $\varepsilon^{Mn}/\varepsilon_0^{Mn}$  reflects mainly the difference in the opening  $T$  of the window support grids. The calculated efficiencies for Al-K and Zr-L from 10- and 30-kV data should be the same.

Generally, peak deconvolution to get line intensities was avoided. However, in case of Mn-L, the  $L\alpha\beta$  and  $L\eta$  contributions are influenced to a different extent by detector icing or a thin oxide layer on the RM surface. Therefore, the related  $\varepsilon^i$  was calculated from the Mn- $L\alpha\beta$  intensity ratio after Mn-L deconvolution.

Equation (5) was used to give the efficiency  $\varepsilon^i$  for nine discrete energies corresponding to the nine most intense characteristic lines in the 10-kV and 30-kV spectra. To get the efficiency as a continuous function for this wide range,

equation (2) with thicknesses as free parameters was fitted to the nine  $\varepsilon^i$  values. A nonlinear least squares fit algorithm with constraints was used. Lower boundaries for the mass thickness of window materials were derived from transmission measurements of Moxtek windows (Scholze & Procop, 2005). The fit does not depend on the MACs in use. Different MACs are balanced by different mass thicknesses in equations (1) and (2). Parameters with negligible influence on the efficiency were kept constant (e.g., nitrogen mass thickness of the window, crystal thickness in case of Si(Li)). Because the efficiency should be known from the very beginning for optimum background construction, an iterative procedure for background construction and efficiency fit was included in the computer program to get the final result. The quality of the fit has proven to be an indicator for correct assumption on detector construction. Starting with the wrong contact material (Au instead of Ni or vice versa) will never end in a good fit of the efficiency curve to the nine  $\varepsilon^i$ . The quality of the background subtraction is also an indicator for correct or incorrect assumptions.

The 10-kV and 30-kV reference spectra are ideally measured at an TOA = 35° with perpendicular electron incidence. Many SEMs have an EDS port with an elevation angle of 35°. Where the unknown spectrometer operates under another TOA, we have demonstrated that measured intensities can be transformed to TOA = 35° using an appropriate X-ray absorption correction procedure. It has also been demonstrated that in case of SEM ports with elevation angles of 30° or 40° the specimen may be tilted to achieve TOA = 35°. The small tilt has negligible impact on X-ray generation within the specimen. This can be verified by the equations for the backscattering factor in case of tilted specimens (Pouchou et al., 1990).

The methodology has been tested by a mutual efficiency determination of the calibrated spectrometers. Spectra of the same specimen have been measured at 10 kV and 30 kV with all four calibrated spectrometers using different SEMs in different laboratories. Detectors were retracted as far as possible to get a small solid angle and hence to minimize any shadowing effect by the window support. This corresponds with the experimental conditions at calibration with SR. Manufacturing details (window type, crystal design) were known in this case. Figure 7 shows the efficiency of one calibrated spectrometer considered here to be the unknown spectrometer derived from the efficiency of a second calibrated spectrometer considered to be the reference spectrometer. The low energy efficiencies of these two spectrometers are rather different because the detector of the reference spectrometer has an Au front contact, whereas the other one has a Ni front contact. The triangles in the figure represent the nine  $\varepsilon^i$  values found from equation (5) for the couples of 10-kV and 30-kV spectra and assuming for normalization a typical value of 0.77 for the geometrical transparency  $T$  of the window of the unknown spectrometer. The solid line is the efficiency curve fitted to these values (mean values from 10- and 30-kV data were taken for

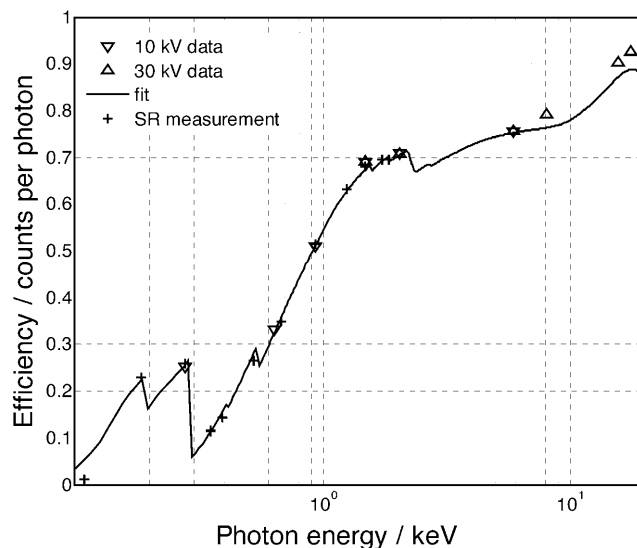


**Figure 7.** Calculated efficiencies  $\varepsilon^i$  from equation (5) (triangles), fitted efficiency curve (solid line), and directly measured efficiency data (crosses) for a spectrometer with Moxtek AP3.3 window and a Si(Li) diode with Au front contact.

Al-K and Zr-L). The crosses give the efficiency of the unknown spectrometer directly measured with monochromatic SR. The mean deviation between the nine  $\varepsilon^i$  and the fitted efficiency curve at these energies is 1.3%. The mean deviation between the 13 directly measured efficiencies (the value with the monochromator setting at 0.108 keV was ignored) and the fitted efficiency for the related energies is 2.5%. This means that the efficiency of the “unknown” spectrometer could be reproduced with an uncertainty below the targeted 5% level. This excellent result of mutual reproduction of efficiency for these two spectrometers could not be achieved for all four calibrated spectrometers. With the spectrometer, which has shown the inconsistency in efficiency calibration mentioned above, set as the reference spectrometer, the low energy efficiencies for the two spectrometers in Figure 7 are either by about 15% too high or too low depending on which of the calibration data are used as reference. Taking the SDD as the unknown spectrometer, the  $\varepsilon^i$  obtained for all but the C-K line were consistent with the calibration using SR. For the SDD type used here, high shelf of low energy lines compromised the net-intensity determination, especially for the C-K line. This problem should no longer be present for new generations of SDDs.

As a field demonstration, the RM-based efficiency transfer was tested in six laboratories equipped with different types of the SEM and EDS. Because the spectrometers involved were not independently calibrated, we cannot be sure of the true efficiency. But the efficiency determined by the proposed methodology gave reasonable results with only one exception, where we established that an old SEM gave incorrect high voltages. Therefore, the check of correct

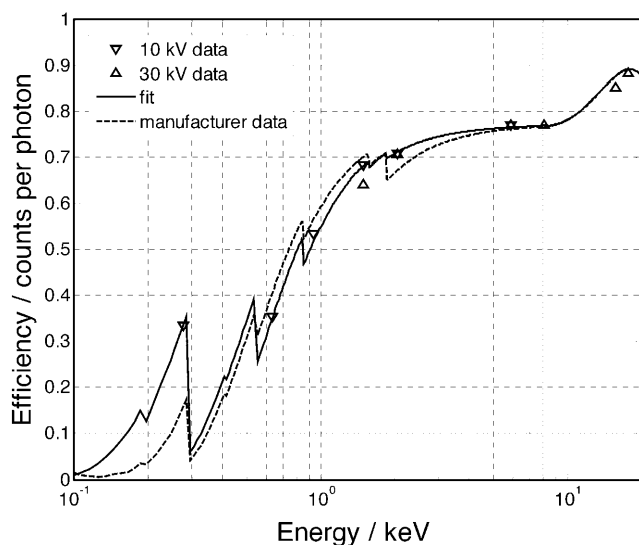


**Figure 8.** Efficiency of a spectrometer with Moxtek AP3.3 window, Si(Li) with Ni front contact, and some icing. The dotted line is calculated with the typical window transmission and with the manufacturer's default settings for the thickness of the front contact and dead layer.

microscope high voltage using the Duane–Hunt law was included in the general procedure for the efficiency transfer. In two of the tested cases, the default settings for the contact material resulted in nonzero values in peak-free regions after background removal and in an extremely poor fit of the  $\varepsilon^i$ . With the true contact material, later confirmed on request by the manufacturers, the actual spectrometer efficiency could be determined. In another case, shown in Figure 8, the efficiency at low energies was much higher than could be expected from the dead layer thickness given in the manufacturer's default setting. For the same spectrometer, the efficiency transfer procedure indicated an icing of the detector. The thickness of that ice layer was confirmed by the determination of the height of the O-K absorption edge in a germanium background spectrum, a method for contamination detection proposed previously (Procop, 1999).

## DISCUSSION

This article proposes a method to get instrumental parameters necessary for the spectrometer in use to perform an analysis. The method consists in principle of the measurement of characteristic properties of an RM by means of a spectrometer, for which the instrumental parameters are well known by a traceable calibration, and to deduce the unknown instrumental parameters performing the same measurement with the spectrometer in use. This kind of approach has been applied in many spectroscopic methods. An example very similar to that described here is the deter-

mination of the transmission function of an electrostatic energy analyzer of an Auger or photoelectron spectrometer by means of an RM, for which the spectra were measured with a calibrated spectrometer and specified (Seah & Smith, 1990). In that example the transmission function is a continuous function, and the most important requirement for the RM is to have an electron spectrum with many lines distributed over the whole energy range.

The same approach to determine the efficiency of an energy dispersive spectrometer is more complicated. The efficiency has discontinuities at absorption edges caused by the detector components. An appropriate RM should have a spectrum with lines close to the edges. In this way, the line intensities are sensitive to changes in the height of absorption edges. A stoichiometric compound that meets the requirements for the RM defined at the beginning of the article could not be found. Finally, we prepared it as a thick (about 10  $\mu\text{m}$ ) hard coating on steel substrates. The RM has nine intensive X-ray lines. They span the wide energy range from 0.28 to 17.67 keV and are used for the efficiency transfer. For that transfer a user needs the RM together with a data sheet containing the six values  $\varepsilon_0^i/(I_0^i/I_0^{Mn})$  from the 10-kV spectrum (C-K to Mn-K $\alpha$ ) and the six values  $\varepsilon_0^i/(I_0^i/I_0^{Mn})$  from the 30-kV spectrum (Al-K to Zr-K $\beta$ ) measured with the calibrated spectrometer at a SEM with a 35° port. From the measured line intensities the user will get nine  $\varepsilon^i$  values for his or her own equipment, whereas two of them (Al-K, Zr-L) are the mean values from the 10- and 30-kV measurement. These nine values reveal the true efficiencies. They have a measurement uncertainty, but no assumption has been made up to this point about detector construction and energy dependence of the efficiency. Only the next step, the determination of the efficiency for the whole energy range, supposes a physical model described by equation (2). For the fit, a data set for the MACs has to be selected. This selection does not influence the fitted efficiency curve, but only the mass thicknesses. This was recently demonstrated for window transmissions measured with monochromatic synchrotron radiation (Scholze & Procop, 2005). In this article, the MACs from CXRO (Henke et al., 1993) with modifications in the absorption edges of carbon and oxygen were used.

When the user places his detector at a short distance from the specimen to get a large solid angle for detection, the radiation emitted nonparallel to the lamellas of the window grid will be partially absorbed. The  $\varepsilon^i$  values will reflect the shadowing effect. The optimum fit by equation (2) will compensate for this by modified parameters. The efficiency is then correct for the given experimental conditions.

There is no line in the region between the carbon and oxygen absorption edges that could fix the efficiency in this energy interval. This is not a problem of RM preparation. Carbon–nitride layers have also been deposited using magnetron sputtering. It is the problem of the limited spectrometer resolution. With the N-K line between C-K and Mn-L, there is no peak-free region for background scaling, and for

some spectrometers even a peak deconvolution would be necessary. Therefore, increased uncertainty in peak area determination would override the advantage of an additional line. However, in the case of a microcalorimetric EDS, that additional line could be exploited.

The accuracy of the efficiency transfer under optimum conditions was studied and found to be as expected within the inevitable measurement uncertainty in spectrometer calibration and spectrum analysis. Optimum conditions mean that absorbing detector components are known and the operation of the SEM including stage and vacuum conditions is correct. The uncertainty in efficiency determined for an unknown (concerning layer thicknesses) spectrometer is below 5% in the energy range below 10 keV. For the energy range above 10 keV, the low intensity of the synchrotron radiation at BESSY II with a critical energy of 2.5 keV limited the accuracy of the reference spectrometer calibration due to poor counting statistics. Meanwhile, the accuracy of efficiency calibration at energies above 10 keV has been considerably improved by using a wavelength shifter. Measurements with monochromatic radiation up to 60 keV and undispersed radiation up to 100 keV were presented recently (Scholze et al., 2006).

The knowledge of the detector type and its components is not as critical for the efficiency transfer as it might seem at first glance. The only significant difference in modern Si(Li) detector diodes is the front contact, either about 20 nm Au or 5–10 nm Ni. The absorption at low energies for these two contacts is so different that a false specification can easily be seen after background subtraction as a remaining nonzero background in peak-free regions. The SDDs currently in use, easy to recognize by low Zr-K intensities, have an Al front contact and a very thin dead layer irrelevant for the efficiency (Kemmer et al., 2005). Finally, a HPGe detector can be easily recognized by the edge at 11.1 keV in the background of the 30-kV spectrum caused by the escape of Ge-K photons.

Under the conditions that the SEM and spectrometer correctly operate and that EDS manufacturer-provided quantitation software is correctly tuned with its detector construction, the improvement in standardless analysis by updating the spectrometer efficiency by means of the proposed procedure will be marginal. However, the procedure remains useful for a periodic check for contamination layer buildup or erroneous pulse processing discussed below. In two of the six laboratories visited in the field demonstration the procedure revealed that the contact layer material was set wrong (Au instead of Ni or vice versa). The influence on a quantitative analysis when lines below 2 keV are used would be far from being marginal. Such carelessness during software installation is easily detected by the efficiency transfer procedure. For older systems upgraded with a new crystal and window after a repair or updated with new stand-alone quantification software, the efficiency transfer procedure is a unique means to find the true spectrometer efficiency needed for the algorithm of standardless analysis. SDDs

have been improved continuously in the past years. The development was accompanied by an increase in diode thickness from initially 0.25 mm to presently 0.4 mm. When the actual thickness for the diode in use was not specified or lost, the efficiency transfer procedure with the 10- and 30-kV reference spectra for Si(Li) can determine that thickness.

It should be emphasized once more that the requirements for SEM and EDS performance for successfully applying the efficiency transfer are the same as for the quantitative analysis. When the indicated high voltage or specimen tilt are not the true values, when the spectrometer is not correctly mounted, so that the assumed TOA is not the true one, or when bad vacuum conditions in the microscope cause a rapid growth of surface contamination, the efficiency transfer procedure should not be applied.

At the beginning, this investigation was focused on low energies with the intention of getting the true efficiency determined from the actual absorption of all components in front of the active crystal volume. It was supposed that the energy dependence of the efficiency is always given by equation (1) and equation (2), respectively. However, the calibration of the four spectrometers showed that equations (1) and (2) are an idealization. The pulse processing influences the efficiency too. The difference in low energy efficiency for one of the calibrated spectrometers found by the two measurement methods (undispersed and monochromatic SR) was already mentioned. Another of the calibrated spectrometers lost pulses at high energies, and the measured efficiency did not show the expected rise above 8 keV (see Fig. 1). Such a loss of high energetic events was also observed for some of the six noncalibrated spectrometers tested. Currently, the  $\epsilon^i$  values for Zr-K $\alpha$  and Zr-K $\beta$  are not included into the fit for a spectrometer with a Si(Li). Instead, the crystal thickness given by the manufacturer is taken as a constant.

For some of the spectrometers the  $\epsilon^i$  ( $i = \text{Al-K}$  and Zr-L) determined at 10 and 30 kV did not agree, although the same procedure was applied to all the spectra. It is intended to improve the net peak area determination by a deconvolution of the L series to account for the broader peaks in the 30-kV spectra measured with a shorter shaping time. The loss of low energy events at high count rates should, however, also be considered as a possible reason for the observed differences.

## CONCLUSIONS

The feasibility of efficiency calibration of an unknown EDS system with a relative uncertainty of about  $\pm 5\%$  by means of the spectrum from a reference material and the efficiency of a reference spectrometer is demonstrated. An RM that meets the requirements for EDS efficiency transfer can be prepared as a 10- $\mu\text{m}$ -thick hard coating on steel sub-

strate by reactive cosputtering. The efficiency of reference spectrometers can be measured using synchrotron radiation. The RM is specified by the line intensities in the 10-kV and 30-kV spectra, measured for the RM specimen with a reference spectrometer under  $\text{TOA} = 35^\circ$ , and the RM composition. The line intensities have a direct influence on the efficiency of the unknown spectrometer, but the composition has only an indirect influence when used for background construction and any necessary absorption correction.

Equations (1) and (2) describe the ideal detector behavior. Any influence of electronic pulse processing is not included. In this study, we tested systems in which low or high energy efficiency is reduced well below the efficiency predicted for likely detector parameters, and we suspect this is caused by problems in pulse processing. Whatever the cause of the discrepancy, the RM and related methodology are a unique means to reveal such artifacts and estimate the consequent errors in standardless ED-EPMA.

## ACKNOWLEDGMENTS

The authors thank the technical staff members of BAM, Mrs. Birgid Strauss and Dr. Alexander Dück, and the ENEA staff members for materials characterization. We are grateful to Dr. Peter Willich (Fraunhofer-Institut für Schicht- und Oberflächentechnik Braunschweig), Dr. Xavier Llovet (Universitat de Barcelona), Dr. Wim G. Sloof (Delft University of Technology) and Dr. Michael Mayr (Voest Alpine Stahl Linz GmbH) for electron probe microanalysis, as well as Dr. Wolfgang Bohne (Hahn-Meitner-Institut Berlin) for elastic recoil detection analysis. The support by Mrs. Christine Roberts formerly with Moxtek Corp. is highly appreciated.

The EDS-CRM research project was funded by the Measurement & Testing Activity of the European Community's 5th Framework "Growth" Programme (EC-Research Directorate General) Contract No. G6RD-CT-2002-00851.

## REFERENCES

- BECKHOFF, B., KLEIN, R., KRUMREY, M., SCHOLZE, F., THORNAGEL, R. & ULM, G. (2000). X-ray detector calibration in the PTB radiometry laboratory at the electron storage ring BESSY II. *Nucl Instr Meth A* **444**, 480–483.
- CAMPBELL, J.L., PERUJO, A. & MILLMAN, B.M. (1987). Analytic description of Si(Li) spectral lineshapes due to monoenergetic photons. *X-ray Spectrom* **16**, 195–201.
- GOTO, S. (1993). Response functions of a Si(Li) detector for photon energies from 1 to 10 keV. *Nucl Instrum Meth A* **333**, 452–457.
- HENKE, B.L., GULLIKSON, E.M. & DAVIS, J.C. (1993). X-ray interactions: Photoabsorption, scattering, transmission, and reflection at  $E = 50\text{--}30000$  eV,  $Z = 1\text{--}92$ . *Atomic Data and Nuclear Data Tables* **54**, 181–342. Available at: [http://www-cxro.lbl.gov/optical\\_constants/atten2.html](http://www-cxro.lbl.gov/optical_constants/atten2.html).
- JOY, D. (2002). Improving matrix corrections. *Mikrochim Acta* **138**, 105–113.
- KEMMER, J., WIEST, F., PAHLKE, A., BOSLAU, O., GOLDSTRASS, P., EGGERT, T., SCHINDLER, M. & EISELE, I. (2005). Epitaxy—A new technology for fabrication of advanced silicon radiation detectors. *Nucl Instrum Meth A* **544**, 612–619.
- LOWE, B.G. (2000). An analytical description of low-energy X-ray spectra in Si(Li) and HPGe detectors. *Nucl Instrum Meth A* **439**, 247–261.
- PHILIBERT, J. (1963). A method for calculating the absorption correction in electron probe microanalysis. In *X-Ray Optics and X-Ray Microanalysis, Proceedings of the 3rd International Symposium on X-Ray Optics and Microanalysis*, Pattee, H.H., Cosslett, V.E. & Engström, A. (Eds.), pp. 379–392. New York: Academic Press.
- POUCHOU, J.-L. (1994). Standardless X-ray analysis of bulk specimens. *Mikrochim Acta* **114/115**, 33–52.
- POUCHOU, J.-L., PICOIR, F. & BOIVIN, D. (1990). Further improvements in quantitation procedures for X-ray microanalysis. In *Proceedings of the XII International Symposium on X-Ray Optics and Microanalysis*, pp. 52–59. Cracow, Poland: Academy of Mining and Metallurgy.
- PROCOP, M. (1999). Estimation of absorbing layer thicknesses for an Si(Li) detector. *X-Ray Spectrom* **28**, 33–40.
- REED, S.J.B. (1975). The shape of continuous X-ray spectrum and background corrections for energy-dispersive electron microprobe analysis. *X-Ray Spectrom* **4**, 14–17.
- REED, S.J.B. & WARE, N.G. (1972). Escape peaks and internal fluorescence in X-ray spectra recorded with lithium drifted silicon detectors. *J Phys E Sci Instrum* **5**, 582–584.
- SCHOLZE, F., BECKHOFF, B., KOLBE, M., KRUMREY, M., MÜLLER, M. & ULM, G. (2006). Detector calibration and measurement of fundamental parameters for X-ray spectrometry. *Proc. EMAS 2005 Workshop*, Florence, Italy; *Microchimica Acta*, in press.
- SCHOLZE, F. & PROCOP, M. (2001). Measurement of detection efficiency and response functions for an Si(Li) X-ray spectrometer in the range 0.1–5 keV. *X-Ray Spectrom* **30**, 69–76.
- SCHOLZE, F. & PROCOP, M. (2005). Detection efficiency of energy-dispersive detectors with low-energy windows. *X-Ray Spectrom* **34**, 473–476.
- SCHOLZE, F., THORNAGEL, R. & ULM, G. (1996). Detector calibration at the PTB radiometry laboratory at BESSY. *Nucl Instrum Meth A* **377**, 209–216.
- SCHOLZE, F., THORNAGEL, R. & ULM, G. (2001). Calibration of energy dispersive X-ray detectors at BESSY I and BESSY II. *Metrologia* **38**, 391–395.
- SCHOLZE, F. & ULM, G. (1994). Characterization of a windowless Si(Li) detector in the photon energy range 0.1 to 5 keV. *Nucl Instrum Meth A* **339**, 49–54.
- SCHWINGER, J. (1949). On the classical radiation of accelerated electrons. *Phys Rev* **75**, 1912–1925.
- SEAH, M.P. & SMITH, G.C. (1990). Quantitative AES and XPS—Determination of the electron spectrometer transmission function and the detector sensitivity energy dependencies for the production of true electron emission spectra in AES and XPS. *Surf Interface Anal* **15**, 751–766.
- ULM, G., BECKHOFF, B., KLEIN, R., KRUMREY, M., RABUS, H. & THORNAGEL, R. (1998). The PTB radiometry laboratory at BESSY II electron storage ring. *Proc SPIE* **3444**, 610–621.
- WERNISCH, J. & RÖHRBACHER, K. (1998). Standardless analysis. *Mikrochim Acta Suppl* **15**, 307–316.